

Room-Temperature Spin Crossover Observed for [(TPyA)Fe^{II}(DBQ²⁻)Fe^{II}(TPyA)]²⁺ [TPyA = Tris(2-pyridylmethyl)amine; DBQ²⁻ = 2,5-Di-*tert*-butyl-3,6-dihydroxy-1,4-benzoquinone]

Kil Sik Min,[†] Antonio DiPasquale,[‡] Arnold L. Rheingold,[‡] and Joel S. Miller^{*†}

Department of Chemistry, University of Utah, 315 South 1400 East Street, Room 2124, Salt Lake City, Utah 84112-0850, and Department of Chemistry, University of California, San Diego, La Jolla, California 92093-0358

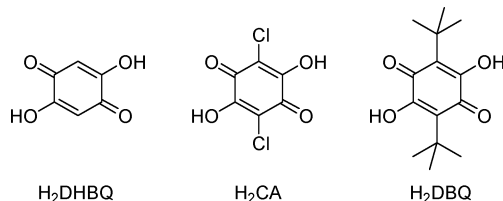
Received December 15, 2006

Dinuclear [(TPyA)Fe^{II}(DBQ²⁻)Fe^{II}(TPyA)](BF₄)₂ possesses extensive π - π interactions between the Fe^{II} dimers that give rise to a two-dimensional supramolecular sheet structure. The magnetic susceptibility shows a room-temperature spin-crossover behavior; however, thermal hysteresis is not observed.

Spin-crossover materials have attracted much attention because of their potential use as a switch or sensor and for data recording.¹ Many Fe^{II} spin-crossover materials have been studied extensively,² and dinuclear Fe^{II} complexes that usually display antiferromagnetic coupling also have been reported to exhibit spin crossover,³ albeit at low temperature. For example, [Fe(phen)(NCS)₂]₂(μ -bpym) (phen = 1,10-phenanthroline; bpym = bipyrimidine; T_c = 170 K).⁴ Thus, it is a challenge to obtain materials with spin transition temperatures around room temperature with hysteresis, although a few Fe^{II} compounds have shown spin-crossover behavior at \sim 290 K and over 325 K.⁵

Metal compounds with 1,4-dihydroxybenzoquinonediide (DHBQ²⁻) and chloranilate (CA²⁻) ligands have been studied because of their redox behavior and magnetism due to the

delocalized π system.⁶ These compounds mainly exhibit weak antiferromagnetic coupling. However, we recently prepared [(TPyA)Fe^{II}(CA)Fe^{II}(TPyA)]ⁿ⁺ [TPyA = tris(2-pyridylmethyl)amine; $n = 2$, CA = CA²⁻; $n = 1$, CA = CA³⁻] bridged with CA²⁻ and spin-bearing CA³⁻ ligands, and they unexpectedly showed intradimer ferromagnetic coupling.⁷ 2,5-Di-*tert*-butyl-3,6-dihydroxy-1,4-benzoquinone (H₂DBQ) with the electron-donating *tert*-butyl group was targeted as a bridging ligand. Herein we report [(TPyA)Fe^{II}(DBQ²⁻)Fe^{II}(TPyA)](BF₄)₂ (**1**) and its room-temperature spin transition.



1 was synthesized from a MeOH solution (50 mL) of [Fe(OH)₂]₆(BF₄)₂ (232 mg, 0.688 mmol) being added to MeOH solutions (10 mL) of TPyA (200 mg, 0.688 mmol) and of H₂DBQ (87 mg, 0.344 mmol). The solution turned dark green, NEt₃ (0.10 mL, 0.688 mmol) was added for neutralization, and the solution was stirred for 1 h at room temperature. After filtration, the solution was concentrated to approximately one-third of the original volume and allowed to stand in a refrigerator for 2 days, whereupon dark-brown microcrystals formed that were collected by filtration, washed with methanol, and dried in vacuo (yield: 200 mg, 52%).⁸

- (5) (a) In *Spin Crossover in Transition Metal Compounds II*; Gütlich, P., Goodwin, H. A., Eds.; Topics in Current Chemistry Vol. 234; Springer: New York, 2004. (b) Rajadurai, C.; Schramm, F.; Brink, S.; Fuhr, O.; Ghafari, M.; Kruk, R.; Ruben, M. *Inorg. Chem.* **2006**, *45*, 10019. (c) Niel, V.; Martinez-Agudo, J. M.; Muñoz, M. C.; Gaspar, A. B.; Real, J. A. *Inorg. Chem.* **2001**, *40*, 3838.
(6) Kitagawa, S.; Kawata, S. *Coord. Chem. Rev.* **2002**, *224*, 11.
(7) Min, K. S.; DiPasquale, A.; Golen, J. A.; Rheingold, A. L.; Miller, J. S. *J. Am. Chem. Soc.* **2007**, *129*, in press.

* To whom correspondence should be addressed. E-mail: jsmiller@chem.utah.edu. Tel.: 1 801 5855455. Fax: 1 801 5818433.

[†] University of Utah.

[‡] University of California, San Diego.

- (1) (a) Kahn, O.; Kröber, J.; Jay, C. *Adv. Mater.* **1992**, *4*, 718. (b) Kahn, O.; Martinez, C. J. *Science* **1998**, *279*, 44. (c) Gaspar, A. B.; Ksenofontov, V.; Seredyuk, M.; Gütlich, P. *Coord. Chem. Rev.* **2005**, *249*, 2661. (d) Gütlich, P.; Garcia, Y.; Goodwin, H. A. *Chem. Soc. Rev.* **2000**, *29*, 419. (e) Muller, R. N.; Elst, L. V.; Laurent, S. J. *Am. Chem. Soc.* **2003**, *125*, 8405.
(2) (a) In *Spin Crossover in Transition Metal Compounds I*; Gütlich, P., Goodwin, H. A., Eds.; Topics in Current Chemistry Vol. 233; Springer: New York, 2004. (b) Real, J. A.; Gaspar, A. B.; Niel, V.; Muñoz, M. C. *Coord. Chem. Rev.* **2003**, *236*, 121.
(3) (a) Létard, J.-F.; Real, J. A.; Moliner, N.; Gaspar, A. B.; Capes, L.; Cadore, O.; Kahn, O. *J. Am. Chem. Soc.* **1999**, *121*, 10630. (b) Ksenofontov, V.; Gaspar, A. B.; Real, J. A.; Gütlich, P. *J. Phys. Chem. B* **2001**, *105*, 12266. (c) Real, A.; Zarembowitch, J.; Kahn, O.; Solans, X. *Inorg. Chem.* **1987**, *26*, 2939.
(4) Batten, S. R.; Bjernemose, J.; Jensen, P.; Leita, B. A.; Murray, K. S.; Moubaraki, B.; Smith, J. P.; Toftlund, H. *Dalton Trans.* **2004**, 3370.

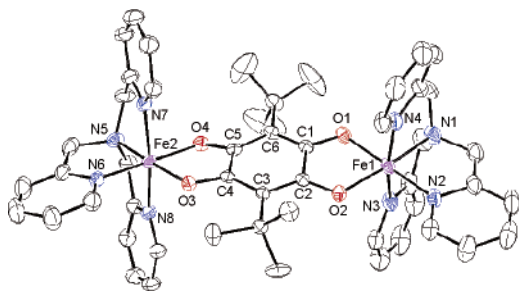


Figure 1. ORTEP (30% probable thermal ellipsoid) view of **1**. H atoms and BF_4^- are omitted for clarity. Relevant distances (\AA) and angles ($^\circ$): At 208 K, Fe1–O1 1.929(3), Fe1–O2 1.929(3), Fe1–N1 1.973(4), Fe1–N2 1.934(4), Fe1–N3 1.959(4), Fe1–N4 1.953(4), Fe2–O3 1.928(3), Fe2–O4 1.933(3), Fe2–N5 1.973(4), Fe2–N6 1.938(4), Fe2–N7 1.957(4), Fe2–N8 1.955(4), C1–C2 1.519(6), C2–C3 1.394(5), C3–C4 1.403(5), C4–C5 1.525(5), C5–C6 1.390(6), C6–C1 1.395(6), C1–O1 1.269(5), C2–O2 1.275(5), C4–O3 1.273(5), C5–O4 1.269(5), O1–Fe1–O2 81.01(13), O3–Fe2–O4 81.08(12). At 298 K, Fe1–O1 1.960(2), Fe1–O2 1.940(2), Fe1–N1 2.014(3), Fe1–N2 1.970(3), Fe1–N3 1.988(3), Fe1–N4 2.004(3), Fe2–O3 1.944(2), Fe2–O4 1.976(2), Fe2–N5 2.036(2), Fe2–N6 1.980(3), Fe2–N7 2.003(3), Fe2–N8 2.012(3), C1–C2 1.518(3), C2–C3 1.404(4), C3–C4 1.400(4), C4–C5 1.530(3), C5–C6 1.400(4), C6–C1 1.390(4), C1–O1 1.272(3), C2–O2 1.280(3), C4–O3 1.272(3), C5–O4 1.266(3), O1–Fe1–O2 80.04(8), O3–Fe2–O4 79.98(8).

Brown block-shaped crystals of **1** suitable for X-ray analysis were obtained by Et_2O diffusion into an acetonitrile solution. The X-ray data were collected at 208 and 298 K, and the ORTEP drawing of **1** is shown in Figure 1.⁹ The structure of the $[(\text{TPyA})\text{Fe}^{\text{II}}(\text{DBQ}^{2-})\text{Fe}^{\text{II}}(\text{TPyA})]^{2+}$ cation shows a distorted octahedral geometry by coordination with the four N atoms of TPyA and the two O atoms of DBQ^{2-} in the cis positions. The average Fe–O and Fe–N bond distances are 1.930(2) and 1.955(1) \AA at 208 K and 1.955(1) and 2.006(1) \AA at 298 K, respectively. The latter is longer than the former by 0.025 and 0.051 \AA because of the increase of the fraction of high-spin Fe^{II} ions as the temperature was increased from 208 to 298 K (vide infra). The cell volume also increases by 150 \AA^3 (2.9%) with increasing temperature. The bond distances relating to Fe–L at 208 K are similar to those found for low-spin Fe^{II} complexes.¹⁰ The average C–O bond distances of DBQ^{2-} are 1.272(3) \AA at 208 K and 1.273(2) \AA at 298 K. The average C–C bond distances (C1–C2

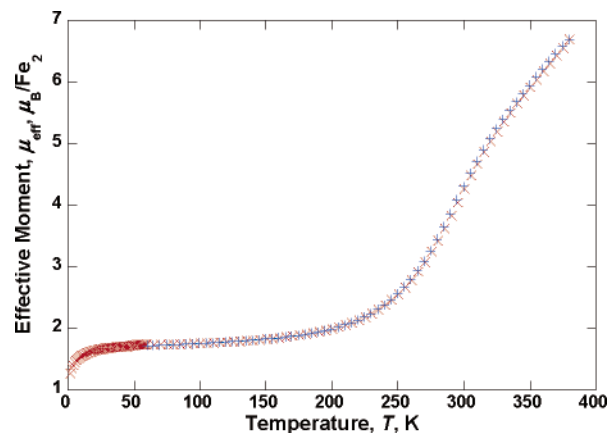


Figure 2. $\mu_{\text{eff}}(T)$ for **1** at 3000 Oe upon warming (\times) and cooling ($+$).

and C4–C5) of DBQ^{2-} are 1.523(4) \AA at 208 K and 1.524(2) \AA at 298 K, indicative of single-bond character, and 1.396 \AA at 208 K and 1.399 \AA at 298 K (C2–C3, C3–C4, C5–C6, and C6–C1), showing that the bonds are delocalized. Based upon the bond distances, the DBQ^{2-} ions at two different temperatures are nearly identical with each other and confirm dianion-bridged ligands, not spin-bearing DBQ^{3-} as described in $[(\text{TPyA})\text{Co}(\text{CA})\text{Co}(\text{TPyA})]^+$.¹¹ The bond distances of Fe–L depend on the temperature, while those of the DBQ^{2-} dianion are temperature-independent.

The pyridyl groups of TPyA ligands and the benzene ring of DBQ^{2-} are involved in C–H $\cdots\pi$ and offset face-to-face π – π interactions between the Fe^{II} dimers,¹² in which the complex gives rise to a two-dimensional supramolecular sheet structure. At 208 K, herringbone structure: H \cdots centroid, 2.64 and 2.73 \AA ; \angle C–H–centroid, 159.20 and 160.40 $^\circ$; centroid \cdots centroid, 4.88 and 4.98 \AA ; dihedral angle, 70.87 and 75.93 $^\circ$. Offset face-to-face: separation, 3.49 \pm 0.05 and 3.23–3.84 \AA ; centroid \cdots centroid, 3.92 and 3.98 \AA ; dihedral angle, 2.24 and 13.44 $^\circ$.

The cyclic voltammogram in acetonitrile displayed three reversible one-electron-transfer waves at $E_{1/2} = +0.802$, $+0.281$, and -1.007 V vs SCE. The former two processes correspond to two successive one-electron oxidations ($\text{1}^{2+/3+}$ and $\text{1}^{3+/4+}$) and the latter to a one-electron reduction ($\text{1}^{2+/+}$). Thus, **1** can be both chemically oxidized and reduced.

The IR spectrum of **1** is temperature-dependent around room temperature, consistent with magnetic data (vide infra). That is, as the temperature decreases below room temperature, the 1501 and 1442 cm^{-1} ν_{CO} peaks decrease and increase in intensity, respectively. At low temperature, a new peak appears at 1467 cm^{-1} . The opposite occurs when the temperature is raised above room temperature. Hence, the IR spectra exhibit an abrupt change at 20 ± 5 $^\circ\text{C}$.

The 2–380 K magnetic susceptibility, χ , was obtained on a SQUID magnetometer (Figure 2). At 380 K, the effective moment, $\mu_{\text{eff}} [= (8\chi T)^{1/2}]$, is 6.69 $\mu_{\text{B}}/\text{Fe}_2$, which decreases with decreasing temperature until it reaches a plateau at ca. 200 K

(8) Characterization of moisture-sensitive **1**. Absorption spectrum (MeOH): λ_{max} , nm (ϵ_{M} , $\text{L mol}^{-1} \text{cm}^{-1}$): 250 (3.7×10^4), 330 (3.6×10^4), 428 (sh, 1.1×10^4), 752 (3.8×10^3). IR (KBr): ν_{CH} 3078 (w), 2951 (m), 1605 (s), 1573 (w), 1502 (vs), 1485 (sh, vs), 1442 (vs), 1335 (s), 1160 (m), 1055 (multiple, br), 905 (m), 763 (s), 655 (m), 521 (m) cm^{-1} . Anal. Calcd for $\text{C}_{50}\text{H}_{54}\text{B}_2\text{F}_8\text{Fe}_2\text{N}_8\text{O}_4$: C, 53.80; H, 4.88; N, 10.04. Found: C, 54.11; H, 5.04; N, 10.19.

(9) Crystal and structure refinement parameters for **1**. At 208(2) K, $\text{C}_{50}\text{H}_{54}\text{B}_2\text{F}_8\text{Fe}_2\text{N}_8\text{O}_4$, fw = 1116.33 g mol^{-1} , monoclinic, space group $P2_1/c$, $a = 15.245(2)$ \AA , $b = 18.481(3)$ \AA , $c = 19.241(3)$ \AA , $\beta = 107.588(2)^\circ$, $V = 5167.4(14)$ \AA^3 , $Z = 4$, $d_{\text{calcd}} = 1.435$ g cm^{-3} , $\mu(\text{Mo K}\alpha) = 0.643$ mm^{-1} , $R1 = 0.0864$, $wR2 = 0.2438$. At 298(2) K, monoclinic, space group $P2_1/c$, $a = 15.398(2)$ \AA , $b = 18.553(2)$ \AA , $c = 19.548(2)$ \AA , $\beta = 107.824(2)^\circ$, $V = 5316.4(9)$ \AA^3 , $Z = 4$, $d_{\text{calcd}} = 1.395$ g cm^{-3} , $\mu(\text{Mo K}\alpha) = 0.625$ mm^{-1} , $R1 = 0.0598$, $wR2 = 0.1782$. Data were collected on a Bruker SMART automatic diffractometer using graphite-monochromated Mo K α ($\lambda = 0.71073$ \AA) radiation. The structure was solved by direct methods and refined by full-matrix least-squares refinement using the *SHELXL97* programs.

(10) (a) Bréfuel, N.; Imatomi, S.; Torigoe, H.; Hagiwara, H.; Shova, S.; Meunier, J.-F.; Bonhommeau, S.; Tuchagues, J.-P.; Matsumoto, N. *Inorg. Chem.* **2006**, *45*, 8126. (b) Törnroos, K. W.; Hostettler, M.; Chernyshov, D.; Vangdal, B.; Bürgi, H.-B. *Chem.–Eur. J.* **2006**, *12*, 6207. (c) Oliver, J. D.; Mullica, D. F.; Hutchinson, B. B.; Milligan, W. O. *Inorg. Chem.* **1980**, *19*, 165.

(11) Min, K. S.; Rheingold, A. L.; DiPasquale, A.; Miller, J. S. *Inorg. Chem.* **2006**, *45*, 6135.

(12) (a) Desiraju, G. R. *Crystal Engineering: The Design of Organic Solids*; Elsevier: New York, 1989; Chapter 4. (b) Shetty, A. S.; Zhang, J.; Moore, J. S. *J. Am. Chem. Soc.* **1996**, *118*, 1019.

COMMUNICATION

($1.99 \mu_{\text{B}}$). Below 200 K, $\chi(T)$ is nearly constant until 30 K. Furthermore, the magnetic moment did not recover to high-spin Fe^{II} ions completely (ca. 93%, $g = 2$) until 380 K and showed a small residual amount of high-spin Fe^{II} ions (3.4%, $g = 2$) at 2 K. Thermal hysteresis, however, was not observed. This is in contrast to $[(\text{TPyA})\text{Co}(\text{DHBQ})\text{Co}(\text{TPyA})]^{3+}$,¹³ which exhibits a thermal hysteresis that is attributed to intermolecular $\pi-\pi$ interactions. **1** also has intermolecular $\pi-\pi$ interactions, but hysteresis was not observed.

Remarkably, **1** shows a spin transition at ~ 300 K as the moment abruptly increases. This behavior is anomalous because most metal complexes with DHBQ and CA exhibit weak antiferromagnetic coupling between paramagnetic species due to the long separation (~ 8.0 Å) and do not exhibit spin crossover.⁶ We have found that the substituents of a bridged ligand (DBQ^{2-}) are very important to inducing

a spin crossover, in which **1** displays spin crossover due to the *tert*-butyl groups. The spin crossover is reproducible. To the best of our knowledge, this is the first example of a dinuclear Fe^{II} complex bridged with a tetraoxolene ligand exhibiting spin crossover around room temperature.

In conclusion, a dinuclear Fe^{II} complex that exhibits spin-crossover behavior around room temperature is reported. Further studies on the redox pressure dependence of the compound and fabrication of new dinuclear complexes showing a hysteresis at room temperature are ongoing.

Acknowledgment. We appreciate the continued partial support of the Department of Energy Division of Material Science (Grant DE-FG03-93ER45504) and of the Army Research Office (Grant DAAD19-01-1-0562).

Supporting Information Available: X-ray crystallographic data in CIF format. This material is available free of charge via the Internet at <http://pubs.acs.org>.

(13) Tao, J.; Maruyama, H.; Sato, O. *J. Am. Chem. Soc.* **2006**, *128*, 1790.

IC062400E